J Mater Sci (2009) 44:6463–6469
DOI 10.1007/s10853-009-3627-0

MESOSTRUCTURED MATERIALS

Synthesis and characterization of mono-dispersed mesoporous spheres

B.-W. Lu · A. Endo · Y. Inagi · A. Harada · T. Ohmori

Received: 28 November 2008 / Accepted: 19 May 2009 / Published online: 16 July 2009

Abstract In the presence of a high TMOS concentration, mono-dispersed mesoporous pure silica spheres with different pore sizes were successfully synthesized using C_{16}TMACl, C_{14}TMACl, and C_{12}TMACl as templates in a methanol–water system, whereas they could not be obtained using C_{10}TMACl. The standard deviation of the particle size prepared with high TMOS concentrations was approximately 10%. Mono-dispersed mesoporous Al-containing spheres could also be synthesized using $NaAlO_2$ as an aluminum source from starting synthesis mixtures with a TMOS/Al ratio of more than 10, but not with a TMOS/Al ratio of less than 8. It was found that the particle size and standard deviation of mono-dispersed mesoporous aluminum-containing spheres depended on the TMOS/Al ratio.

Introduction

Controlling the morphology of mesoporous materials is very important for certain applications and so these materials have been produced in the form of fibers [1–3], rods [4, 5], and spheres [6–15]. Of these morphologies, spheres are very promising for use as reactors, columns [16–19], cosmetics [20], or fixed and fluidized beds. The synthesis of mono-dispersed silica spheres has attracted much attention since they were first synthesized by Stöber and Fink in 1968 [21]. The synthesis of mono-dispersed mesoporous silica spheres was then studied by modifying Stöber's procedure with the addition of alkyl-amine as a template [6, 11, 22, 23]. Recently, mono-dispersed mesoporous silica spheres have been synthesized in the low silica concentration using an alcohol–water system [24–26]. However, when the synthesis was carried out in the presence of low silica concentration, the product yield was very low and a lot of pollutant wastes were formed compared with the synthesis using the precursor solution with high silica concentration.

In addition, the incorporation of heteroatoms in the framework of mesoporous materials by isomorphous substitution is widely employed for designing catalytic sites and improving their hydrothermal stability [27, 28]. Of these metal-substituted mesoporous materials, aluminum (Al)-containing materials have been employed for acid catalyzed alkylation/acylations of aromatics, hydroisomerization, and cracking reactions of bulky molecules [28]. Although the synthesis of mesoporous Al-containing silica spheres with the particle size of 30–50 μm has been reported[29], the standard deviation has not been measured (seems to be larger than 20%), and to the best of our knowledge no one has yet reported the synthesis of mono-dispersed mesoporous Al-containing silica spheres with different Si/Al ratio.

Therefore, to obtain mono-dispersed mesoporous silica spheres with a high yield, we have investigated various synthesis conditions in the presence of high TMOS concentration using a methanol–water system with different surfactants. Moreover, we have attempted to synthesize mono-dispersed mesoporous Al-containing silica spheres with different Si/Al ratio.

Experimental

The starting synthesis mixture for mono-dispersed mesoporous silica spheres with different surfactants was prepared

B.-W. Lu · A. Endo (✉) · Y. Inagi · A. Harada · T. Ohmori
National Institute of Advanced Industrial Science and Technology (AIST), AIST Central 5-2, 1-1-1 Higashi, Tsukuba, Ibaraki 305-8565, Japan
e-mail: endo-akira@aist.go.jp

as follows. Surfactant C_nTMACl (C_{16}TMACl, C_{14}TMACl, C_{12}TMACl, or C_{10}TMACl) was dissolved in 160 g of water/methanol solution with different weight ratios, and then TMOS was added at room temperature. After stirring for 30 min, 1 M NaOH solution or a solution obtained by dissolving $NaAlO_2$ in 1 M NaOH solution was added to obtain a starting synthesis mixture. This starting synthesis mixture was stirred at room temperature for 8 h to prepare pure mesoporous silica and then aged overnight under a static condition, or for 24 h to obtain mesoporous Al-containing silica. The white solid product obtained was centrifuged, filtered, washed thoroughly with deionized water, dried overnight at room temperature, and calcined at 550 °C for 6 h.

XRD patterns were collected with a powder X-ray diffractometer. The bulk chemical compositions were measured by ICP-OES. The morphology was observed with a scanning electron microscope (SEM). Nitrogen adsorption/desorption isotherms at –196 °C were obtained using a conventional volumetric apparatus. The pore size distribution was calculated from desorption branch of nitrogen isotherms using the Broekhoff de Boer (BdB) method [30] with the conventional Dollimore-Heal algorithm. The ^{27}Al MAS NMR spectra of mono-dispersed mesoporous Al-containing spheres calcined at 550 °C were recorded using a 7-mm diameter zirconia rotor on a Bruker Biospin ADVANCE 400 system at 104.2 MHz.

Results and discussion

Mono-dispersed mesoporous pure silica spheres

First, we investigated the effect of various synthesis conditions such as NaOH and surfactant concentration on the formation of mono-dispersed mesoporous silica spheres in the presence of high TMOS concentration using a methanol–water system. The results are given in Table 1, and some SEM images of particles are shown in Fig. 1. When the TMOS concentration was increased (Samples 1 and 2), the particle size slightly increased and the pore volume decreased, whereas the pore diameter was almost constant. Therefore, the increase in the particle size is mainly caused by the increase of the wall thickness of the silica framework. When the NaOH concentration was increased (Samples 2 and 3), the particle size remained almost unchanged. When the surfactant concentration was increased (Samples 3–6), the particle size decreased significantly, but the particle size was unaffected when the concentration was increased further (Samples 6 and 7). The reduction in the particle size may be due to the increase in solution viscosity with the increase in surfactant concentration, resulting in the generation of more nuclei as previously reported [26]. In addition, the standard deviation of mono-dispersed pure silica spheres (Sample 2 or 3) was about 10% even when we used a relatively high surfactant concentration, regardless of the TMOS and NaOH concentrations, whereas the standard deviation was more than 20% when the surfactant concentration was increased further.

Next, with a high TMOS concentration, we attempted to synthesize mono-dispersed pure silica spheres with a high yield, and to investigate the effect of the weight ratio of water/methanol on the formation of mono-dispersed pure silica spheres. The results are also given in Table 1, and a SEM image is shown in Fig. 1. As shown in Table 1, mono-dispersed pure silica spheres could be obtained even at a high TMOS concentration (Sample 8), and the standard deviation was about 10%, showing a better value in comparison with the reported work [25]. When we employed C_{16}TMACl as a surfactant, we found that when the TMOS concentration was high, mono-dispersed pure silica spheres could only be obtained when the MeOH/(H_2O + MeOH) ratio was between 0.45 and 0.50 (Samples 8 and 10). This result indicates that when the TMOS concentration was very high, the range of the MeOH/(H_2O + MeOH) ratio for preparing mono-dispersed pure silica spheres was very narrow, unlike that obtained with a relatively low TMOS concentration [25]. In addition, the particle size decreased with decreases in the MeOH/(H_2O + MeOH) ratio.

Then, in the presence of a high TMOS concentration, mono-dispersed pure silica spheres with different pore sizes were synthesized using different surfactants, namely C_{14}TMACl, C_{12}TMACl, and C_{10}TMACl, and the effect of the MeOH/(H_2O + MeOH) ratio on the formation of mono-dispersed pure silica spheres was also investigated. The results are listed in Table 1, and SEM images are shown in Fig. 1. With a high TMOS concentration, and when C_{14}TMACl and C_{12}TMACl were employed as surfactants, the range of the MeOH/(H_2O + MeOH) ratio for preparing mono-dispersed pure silica spheres was also rather narrow. In addition, the optimum MeOH/(H_2O + MeOH) ratio for obtaining mono-dispersed pure silica spheres decreased with a decrease in the number n in C_nTMACl. When C_{10}TMACl was employed as a surfactant, mono-dispersed pure silica spheres could not be obtained in the presence of a high TMOS concentration even when the MeOH/(H_2O + MeOH) ratio was changed, because more species were present when the C_{10}TMACl concentration was high, which led to the reaction occurring quickly.

The XRD patterns of calcined mono-dispersed pure silica spheres are shown in Fig. 2A. All the patterns had three well-resolved peaks for the (100), (110), and (200) planes, indicating mesoporous hexagonal regularity. As shown in Fig. 2A, the d (100) values decreased with a decrease in n in C_nTMACl. In addition the XRD pattern

Table 1 Synthesis and characterization of mesoporous pure silica spheres

Sample no.	Synthesis conditions					Product					
	C_nTMACl (n)	C_nTMACl/ (H_2O + MeOH) ((Mol/g)*10^{-5})	TMOS/ (H_2O + MeOH) ((Mol/g)*10^{-4})	NaOH/ (H_2O + MeOH) ((Mol/g)*10^{-6})	MeOH/ (MeOH + H_2O) (Wt:Wt)	Shape of particles[a]	Average particle size (μm)	Standard deviation (%)	BET (m^2 g^{-1})	Pore volume (cm^3 g^{-1})	Pore size (nm)
1	16	1.37	0.109	2.8	0.50	MDS	0.71	10.9	1286.2	0.67	2.74
2	16	1.37	0.379	2.8	0.50	MDS	0.98	8.6	924.9	0.51	2.77
3	16	1.37	0.379	5.7	0.50	MDS	0.96	11.4	1187.8	0.68	2.76
4	16	2.73	0.379	5.7	0.50	MDS	0.40	22.9	976.7	0.58	2.76
5	16	4.10	0.379	5.7	0.50	MDS	0.30	22.4	975.5	0.57	2.76
6	16	5.46	0.379	5.7	0.50	MDS	0.25	21.6	969.2	0.57	2.77
7	16	8.19	0.379	5.7	0.50	MDS	0.24	22.1	971.4	0.57	2.77
8	16	2.73	1.085	5.7	0.50	MDS	0.45	9.2	946.6	0.45	2.48
9	16	2.73	1.085	5.7	0.40	S	–	–	837.4	0.46	2.51
10	16	2.73	1.085	5.7	0.45	MDS	0.16	12.6	844.7	0.43	2.51
11	16	2.73	1.085	5.7	0.55	S			848.8	0.40	2.47
12	14	2.73	1.085	5.7	0.30	S	–	–	705.2	0.36	2.16
13	14	2.73	1.085	5.7	0.35	MDS	0.15	11.7	695.6	0.32	2.15
14	14	2.73	1.085	5.7	0.40	MDS	0.33	22.9	885.2	0.39	2.21
15	14	2.73	1.085	5.7	0.45	S	–	–	726.1	0.32	2.14
16	12	2.73	1.085	5.7	0.15	S	–	–	557.8	0.29	2.13
17	12	2.73	1.085	5.7	0.20	MDS	0.15	10.3	653.7	0.31	2.12
18	12	2.73	1.085	5.7	0.25	MDS	0.38	30.6	867.7	0.38	2.08
19	12	2.73	1.085	5.7	0.30	S	–	–	557.7	0.25	1.79
20	10	2.73	1.085	5.7	0.00	I	–	–	224.0	0.29	–
21	10	2.73	1.085	5.7	0.10	IS	–	–	568.7	0.39	–
22	10	2.73	1.085	5.7	0.20	S	–	–	531.9	0.31	–
23	10	2.73	1.085	5.7	0.50	I	–	–	578.7	0.54	1.77

[a] *MDS* Mono-dispersed sphere, *S* sphere, *I* irregular, *IS* irregular and sphere

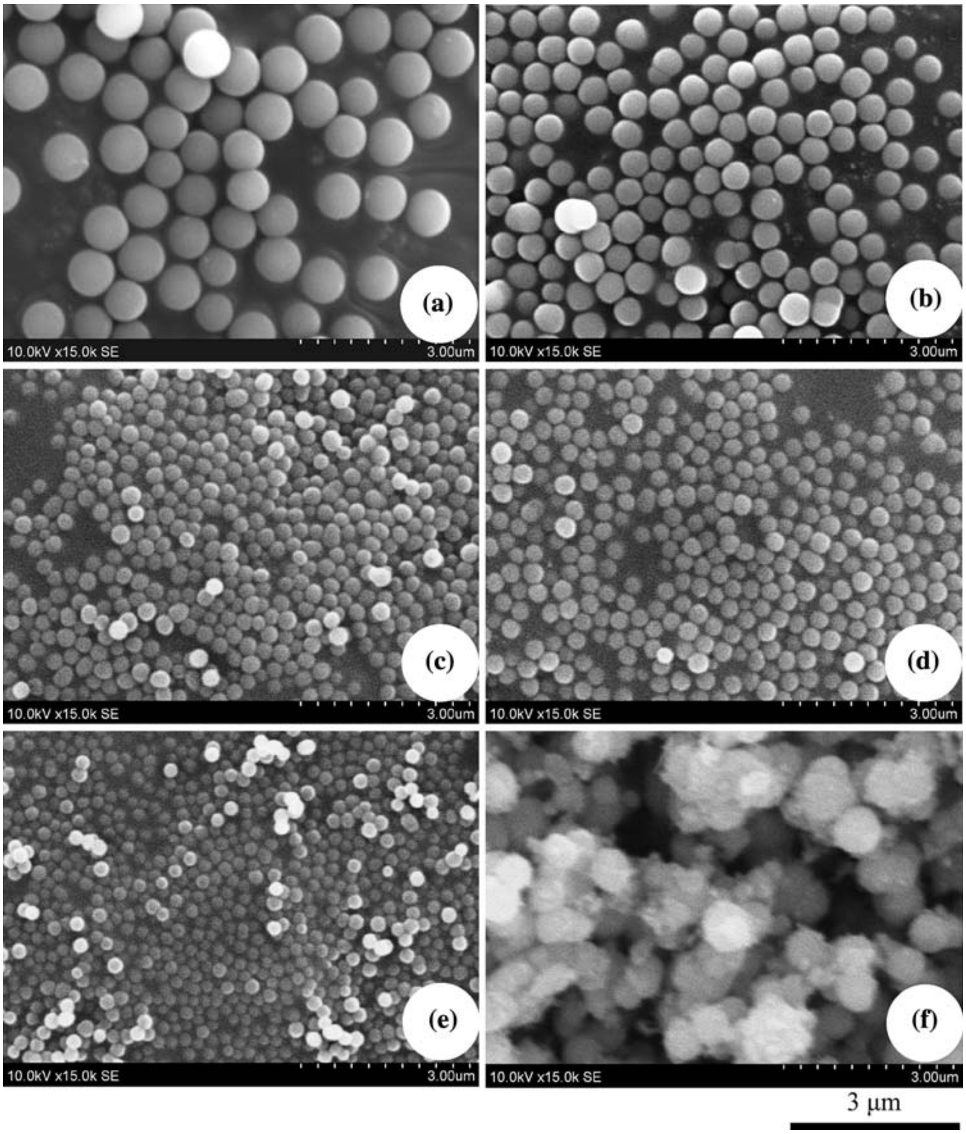

Fig. 1 SEM images of various mono-dispersed mesoporous pure silica spheres. Samples: (**a**) 1, (**b**) 8, (**c**) 10, (**d**) 13, (**e**) 17, (**f**) 21

(Fig. 2A(b, c)) of mono-dispersed pure silica spheres synthesized with a high TMOS concentration was the same as the XRD pattern (Fig. 2A(a)) obtained in the presence of a low TMOS concentration. Figure 2B shows the nitrogen adsorption/desorption isotherms obtained for the mono-dispersed pure silica spheres. The isotherms were similar to type IV in the IUPAC classification [31], clearly indicating that they have a mesoporous structure. Although there was almost no difference in pore size, the specific surface area and pore volume were dependent on the NaOH/TMOS ratio (Samples 1 and 2), and increased with an increase in the NaOH/TMOS ratio. Even for the mono-dispersed pure silica spheres obtained at a high TMOS concentration (Fig. 2B(b, c)) there was no difference in the shape of the nitrogen adsorption/desorption isotherms compared with those of the sample (Fig. 2B(a)) in that they had a high specific surface area and a large pore volume. In addition, the specific surface area, pore volume, and pore size decreased with decreases in n in C_nTMACl. The pore size of mono-dispersed mesoporous silica spheres can be controlled by using C_nTMACl with different alkyl-chain lengths even from a thick starting solution.

Mono-dispersed mesoporous Al-containing silica spheres

To obtain mono-dispersed mesoporous Al-containing spheres, we attempted to incorporate aluminum into a mesoporous siliceous framework using $NaAlO_2$ as an aluminum source. The results are listed in Table 2, and some SEM images of particles are shown in Fig. 3. The Si/Al ratio in the resulting mono-dispersed mesoporous Al-containing silica spheres was measured with the ICP-OES analysis technique. We found that the Si/Al ratio in the product agreed with the

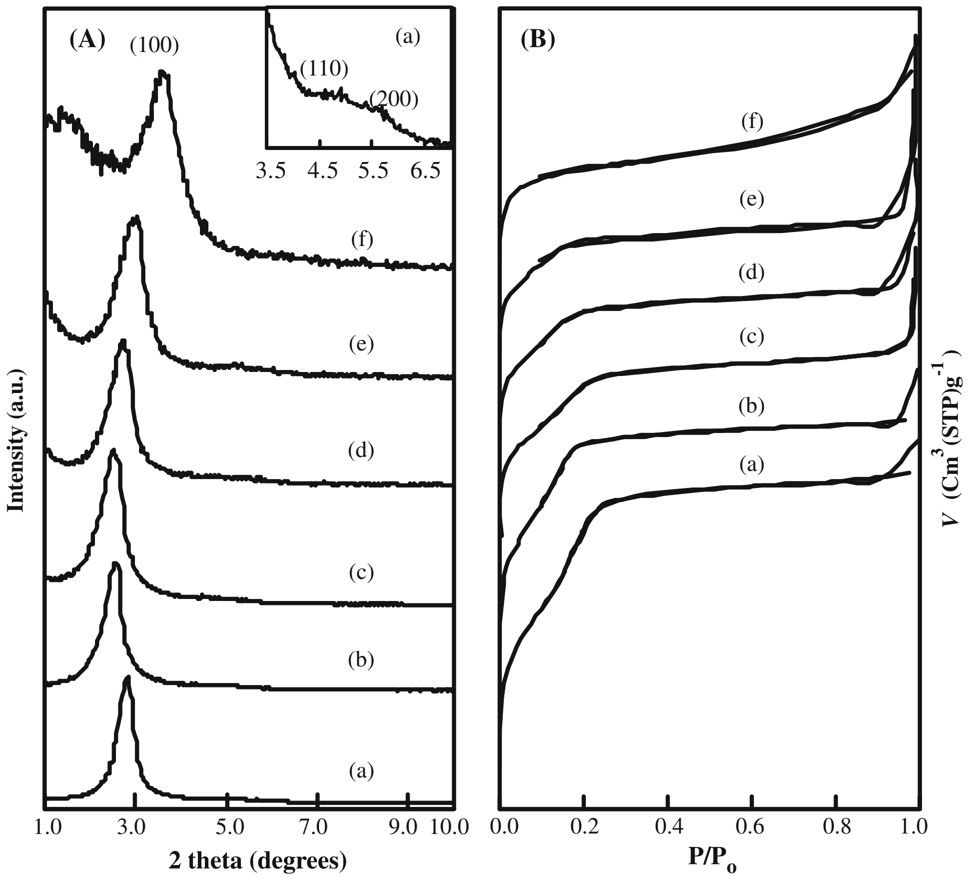

Fig. 2 **A** XRD patterns and **B** nitrogen adsorption–desorption isotherms of various mono-dispersed mesoporous pure silica spheres. Samples: (*a*) 1, (*b*) 8, (*c*) 10, (*d*) 13, (*e*) 17, (*f*) 21

Table 2 Synthesis and characterization of mesoporous Al-containing silica spheres with C_{16}TMACl

Sample no.	Synthesis conditions	Product							
	NaOH/TMOS	TMOS/Al	Si/Al	Shape of particles[a]	Average particle size (μm)	Standard deviation (%)	BET (m^2 g^{-1})	Pore volume (cm^3 g^{-1})	Pore size (nm)
24	0.037	8.0	–	S	–	–	1142.9	0.48	2.25
25	0.075	8.0	–	IS	–	–	1209.8	0.50	2.14
26	0.075	10.0	10.3	MDS	0.92	35.6	1305.7	0.55	2.39
27	0.075	13.3	13.6	MDS	0.69	22.9	1313.5	0.57	2.46
28	0.075	20.0	21.1	MDS	0.51	20.4	1186.5	0.61	2.56
29	0.075	30.0	31.0	MDS	0.42	10.1	1190.9	0.61	2.56
30	0.075	40.0	48.6	MDS	0.54	9.3	1087.6	0.57	2.58
31	0.075	50.0	57.5	MDS	0.54	9.5	1089.6	0.59	2.66

MeOH/(MeOH+H_2O) (Wt/Wt) = 0.5, C_{16}TMACl/TMOS = 0.362

[a] *MDS* Mono-dispersed sphere, *S* sphere, *I* irregular, *IS* irregular and sphere

TMOS/Al ratio in the starting synthesis mixtures when the TMOS/Al ratio was less than 30. However, there was a slight difference in the Si/Al ratio between the product and the starting synthesis mixtures when the ratio was more than 30. Although mono-dispersed mesoporous Al-containing silica spheres could be obtained when the TMOS/Al ratios in the starting mixtures were more than 10, they could not be obtained when the TMOS/Al ratio was less than 8 even if the NaOH/TMOS ratio was changed (Samples 24, 25). This indicates that the formation of mono-dispersed mesoporous Al-containing silica spheres is closely related to the TMOS/Al ratio, namely the TMOS/Al ratio affected the morphology of the obtained mesoporous Al-containing silica.

The XRD patterns of calcined mono-dispersed mesoporous Al-containing silica spheres are shown in Fig. 4A. All the patterns had three well-resolved peaks for the (100), (110), and (200) planes, regardless of aluminum incorporation, indicating mesoporous hexagonal regularity. In

Fig. 3 SEM images of various mono-dispersed mesoporous silica spheres containing aluminum. Samples: (**a**) 25, (**b**) 26, (**c**) 29, (**d**) 31

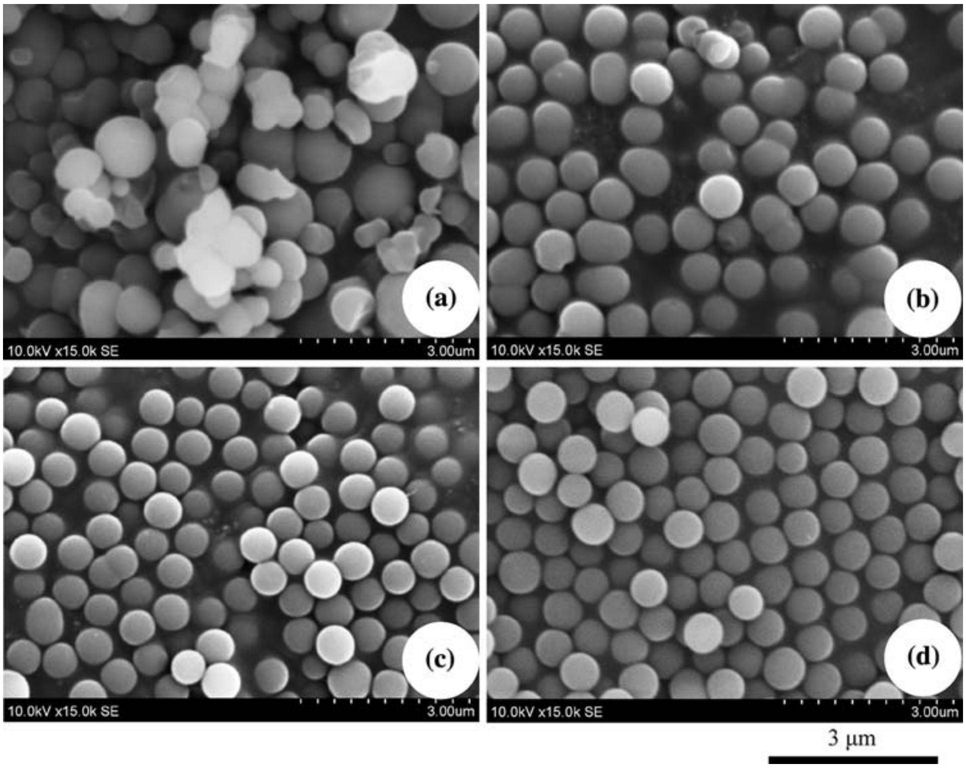

Fig. 4 **A** XRD patterns and **B** nitrogen adsorption–desorption isotherms of various mono-dispersed mesoporous Al-containing silica spheres. Samples: (*a*) 25, (*b*) 26, (*c*) 29, (*d*) 31

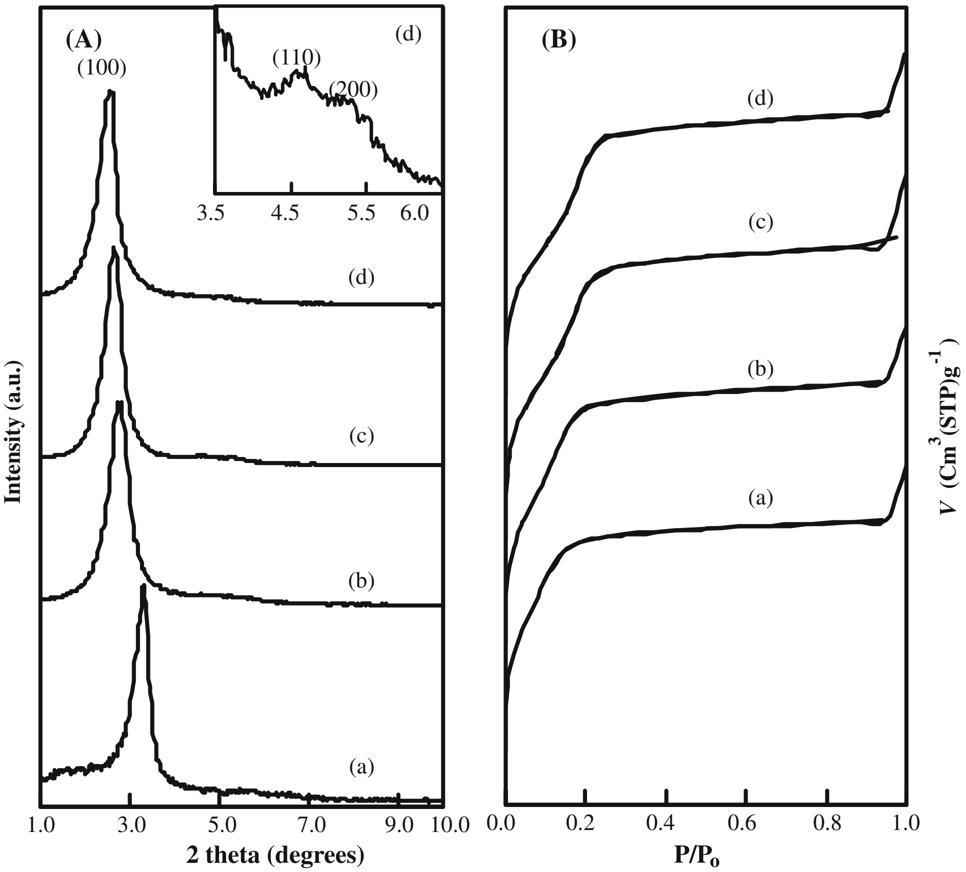

addition, the *d* (100) values decreased with decreases in the TMOS/Al ratio, indicating that aluminum was incorporated into the mesoporous framework, which resulted in a reduction in the distance between pore centers [32]. Figure 4B shows the nitrogen adsorption/desorption isotherms of the obtained mono-dispersed mesoporous Al-containing silica spheres. The isotherms were similar to type IV in the IUPAC classification [31], indicating clearly that the spheres have a mesoporous structure. As shown in Table 2, it is very clear that all the Al-containing samples had a higher specific surface area and a larger pore volume than the pure silica sample. When the TMOS/Al ratio in the starting synthesis mixtures was more than 20, the pore size of the Al-containing samples was almost the same as that of the siliceous sample, whereas it was smaller when the TMOS/Al ratio in the starting synthesis mixtures was from 10 to 20, indicating a decrease in the structure ordering compared with the siliceous sample.

As shown in Table 2, we found that the particles size was greatly affected by the TMOS/Al ratio in the starting synthesis mixtures. Although the particle sizes of the mesoporous Al-containing samples were smaller than those of the pure silica samples, perhaps owing to the fact that more nuclei are generated when the aluminum species was present in starting synthesis mixtures, the particle size obtained from the starting synthesis mixtures with a TMOS/Al ratio of 30 was the smallest. When the TMOS/Al ratio in the starting synthesis mixtures was more than or less than 30, the particle size increased with increases or decreases in the TMOS /Al ratio. As shown in Table 2, it is very interesting to note that the standard deviation was also influenced by the TMOS/Al ratio in the starting synthesis mixtures. The standard deviation was approximately 10% when the particles were obtained from starting synthesis mixtures with a TMOS/Al ratio of more than 30, whereas it was more than 20% when they were obtained from mixtures with a TMOS/Al ratio of less than 30.

Conclusion

Mono-dispersed mesoporous pure silica spheres with a high yield could be obtained successfully using different surfactants. We found that in the presence of a high TMOS concentration, the optimum MeOH/(H_2O + MeOH) ratio for obtaining the mono-dispersed pure silica spheres was very narrow and depended on the carbon chain length of the template surfactant. When aluminum was incorporated in a mesoporous siliceous framework, mono-dispersed mesoporous Al-containing spheres could only be obtained from starting synthesis mixtures with a TMOS/Al ratio of more than 10, and the particle sizes were smaller than those of pure silica samples. In addition, the particle sizes and standard deviations of the mesoporous Al-containing samples depended on the TMOS/Al ratio.

References

1. Yang P, Zhao D, Chemlka BF, Stucky GD (1998) Chem Mater 10:2033
2. Bruinsma PJ, Kim AY, Liu J, Baskaran S (1997) Chem Mater 9:2507
3. Sayari A, Jaroniec M, Pinnvaia TJ (eds) (2000) Nanoporous materials II: studies in surface science and catalysis, vol 129. Elsevier, Amsterdam, p 7
4. Shio S, Kimura A, Yamaguchi M, Yoshida K, Kuroda K (1998) Chem Commun 2461
5. Kosuge K, Sato T, Kikukawa N, Takemori M (2004) Chem Mater 16:899
6. Qi L, Ma J, Cheng H, Zhao Z (2000) Stud Surf Sci Catal 129:37
7. Blin JL, Leonard A, Su BL (2001) Chem Mater 10:3772
8. Yang H, Vovk G, Coombs N, Sokolov I, Ozin GA (1998) J Mater Chem 8:743
9. Boissiere C, Lee A, Mansouri AE, Larbot A, Prouzet E (1999) Chem Commun 2047
10. Schumacher K, Grun M, Unger KK (1999) Microporous Mesoporous Mater 27:201
11. Grun M, Lauer I, Unger KK (1999) Adv Mater 9:254
12. Lu Y, Fan H, Stump A, Ward TL, Rieker T, Brinker CJ (1999) Nature 398:223
13. Schacht S, Huo Q, Voigt-Martin IG, Stucky GD, Schuth F (1996) Science 273:768
14. Fowler CE, Khushalani D, Mann S (2001) Chem Commun 2028
15. Kosuge K, Singh PS (2001) Microporous Mesoporous Mater 44–45:139
16. Boissiere C, Kummel M, Persin M, Larbot A, Prouzet E (2001) Adv Funct Mater 11:129
17. Gallis KW, Araujo JT, Duff KJ, Moore JG, Landry CC (1999) Adv Mater 11:1452
18. Kurganov A, Unger KK, Issaeva T (1996) J Chromatogr A 753:177
19. Nassivera T, Eklund AG, Landry CC (2002) J Chromatogr A 973:97
20. Lee M-H, Oh S-G, Moon S-K, Bae S-Y (2001) J Colloid Interface Sci 83:240
21. Stober W, Fink A (1968) J Colloid Interface Sci 26:62
22. Grun M, Buchel G, Kumar D, Schumacher K, Bidlingmajer B, Unger KK (2000) Stud Surf Sci Catal 128:155
23. Schumacher K, Renker S, Unger KK, Ulrich R, Chesne AD, Spiess HW, Wiesner U (2000) Stud Surf Sci Catal 129:1
24. Yano K, Fukushima Y (2003) J Mater Chem 13:2577
25. Yano K, Fukushima Y (2004) J Mater Chem 14:1579
26. Yamada Y, Yano K (2006) Microporous Mesoporous Mater 93:190
27. Sayali A (1996) Chem Mater 8:1840
28. Corma A (1997) Chem Rev 97:2373
29. Kosuge K, Singh PS (2001) Chem Mater 13:2476
30. Broekhoff JCP, de Boer JH (1968) J Catal 10:377
31. Gregg SJ, Sing KSW (1982) Adsorption surface area and porosity. Academic Press, New York
32. Shen S-C, Kawi S (1999) J Phys Chem B 103:8870